miR-491-3p functions as a tumor suppressor in non-small cell lung cancer by targeting fibroblast growth factor 5

GAI ZHANG[1,2], HAIJIAN ZHENG[1] and LING WANG[1]

[1]Department of General Medicine, The First Affiliated Hospital of Soochow University, Suzhou, Jiangsu 215006; [2]Department of Emergency Medical, The First Affiliated Hospital of Wannan Medical College Yijishan Hospital, Wuhu, Anhui 241006, P.R. China

Received February 25, 2022; Accepted May 4, 2022

DOI: 10.3892/or.2022.8379

Abstract. The present study aimed to identify the function of miR-491-3p in regulating non-small cell lung cancer (NSCLC). Tumor tissues and adjacent normal tissues were collected from 43 patients with NSCLC. A549 and H1299 cells were transfected with microRNA (miR)-491-3p mimic, mimic negative control (NC), miR-491-3p inhibitor, inhibitor NC, pcDNA3.1-FGF5 vector and control vector. Cell counting kit-8 assay and Edu experiments were performed to assess cell viability and proliferation. Matrigel experiment, wound healing assay and flow cytometric analysis were performed to explore cell invasion, migration and apoptosis, respectively. A dual-luciferase reporter experiment was performed to identify the relationship between miR-491-3p and fibroblast growth factor 5 (FGF5). *In vivo* study was conducted by using nude mice. The miR-491-3p and FGF5 protein expression levels were investigated using reverse transcription-quantitative polymerase chain reaction and western blot analysis. In NSCLC tumor tissues, miR-491-3p was downregulated and FGF5 was upregulated (P<0.01). Low miR-491-3p expression and high FGF5 mRNA expression was associated with poor outcomes in patients, including advanced TNM stage and lymph node metastasis (P<0.05). upregulation of miR-491-3p suppressed viability, proliferation, invasion and migration of NSCLC cells; however, it promoted apoptosis (P<0.01). FGF5 was a target gene for miR-491-3p. miR-491-3p directly inhibited FGF5 expression. upregulation of FGF5 significantly reversed the inhibitory effects of miR-491-3p on malignant phenotypes of NSCLC cells (P<0.01). miR-491-3p overexpression suppressed the *in vivo* growth of NSCLC. Thus, it was identified that miR-491-3p functions as a tumor suppressor in NSCLC by directly targeting FGF5.

Correspondence to: Dr Ling Wang, Department of General Medicine, The First Affiliated Hospital of Soochow University, 899 Pinghai Road, Suzhou, Jiangsu 215006, P.R. China
E-mail: sudawangling1111@163.com

Key words: non-small cell lung cancer, microRNA-491-3p/fibroblast growth factor 5, proliferation, invasion, apoptosis

Introduction

Lung cancer is one of the most common malignant tumors and ~25% of all cancer-related deaths are related to lung cancer (1). Lung cancer can be divided into small cell lung cancer and non-small cell lung cancer (NSCLC) according to its histopathological features (2). The proportion of NSCLC cases is 80-85% of all the lung cancer cases (3). In the past decades, several effective novel strategies have been emerged in NSCLC treatment research, such as immunotherapy (4). Moreover, anti-angiogenic agents have been also discovered to improve the outcomes of patients with NSCLC (5). Previously, drug-loaded nanoparticle treatment and nanotechnology drug delivery strategies in the lungs have been reported to be effective in the treatment of lung cancer (6-8). However, the 5-year survival rate is only ~20% despite improved treatment methods (2). exploration and elucidation of its molecular mechanisms is key to improving the prognosis.

MicroRNAs (miRNAs or miRs) are a class of non-coding small RNAs (9). They play a crucial role in regulating biological processes, such as apoptosis, invasion, autophagy and proliferation (10,11). miR-491-3p plays an indispensable role in regulating development in certain human tumors. For instance, invasion, migration, and proliferation were weakened and apoptosis was exacerbated in retinoblastoma cells after miR-491-3p was upregulated (12). miR-491-3p acts as a tumor suppressor in osteosarcoma by inhibiting the growth and invasion of the osteosarcoma cells (13). Zhao *et al* (14) showed that miR-491-3p attenuated the multidrug resistance of hepatocellular carcinoma. Simultaneously, low miR-491-3p expression was associated with poor outcomes in patients with tongue cancer. The inhibition of miR-491-3p expression enhanced the chemotherapy resistance of the tongue cancer cells (15). However, the role of miR-491-3p in NSCLC remains unclear. In our preliminary research (Fig. 1A), it was found that miR-491-3p expression was abnormally low expressed in patients with NSCLC. Therefore, it was hypothesized that miR-491-3p may be involved in regulating the progression of NSCLC. The present study was then executed to identify the function of miR-491-3p in NSCLC progression.

It has been revealed that one of the main ways of miRNAs to regulate diseases development is to regulate coding genes expression via binding to specific mRNA targets (16). through

TargetScan version 7.1 (http://www.targetscan.org/vert_71/) prediction, it was observed that fibroblast growth factor 5 (FGF5) had the binding site for miR-491-3p in the 3'-untranslated (UTR) region. Notably, our preliminary research (Fig. 1B) indicated that FGF5 was aberrantly up-regulated in patients with NSCLC. FGF5 has been reported to be overexpressed in NSCLC. The silencing of FGF5 reduced proliferation, migration and invasion and enhanced apoptosis in NSCLC cells (17). Moreover, high FGF5 expression was reported to be associated with poor overall survival and relapse-free survival patients with in lung adenocarcinoma (18). Taking together, it was hypothesized that miR-491-3p may regulate NSCLC progression by targeting FGF5. In the present study, a series of experiments were performed to identify this hypothesis. The present findings may provide a novel molecular target for NSCLC treatment.

Materials and methods

Patients and tissues. Patients with NSCLC (n=43) from Yijishan Hospital (Wuhu, China) participated in the present study. Patients with previous history of cancer-related treatments were not included. Patients with other severe organic diseases were excluded. All patients with NSCLC were treated with surgical resection from April 2018 to November 2019 at the First Affiliated Hospital of Wannan Medical College Yijishan Hospital (Wuhu, China). tumor tissues and adjacent normal tissues were collected and stored in liquid nitrogen. Clinicopathological characteristics of all the patients were recorded. The research protocol was reviewed and approved (approval no. TCH036) by the Ethics Committee of the First Affiliated Hospital of Wannan Medical College Yijishan Hospital (Wuhu, China) and was in line with the Declaration of Helsinki. Written informed consent was obtained from all patients. Details of all were de-identified patients. The document of the Ethics Committee was related to the human studies of the present study.

Cell culture and transfection. A549 (CCL-185) and H1299 cells (CRL-5803) were commercially obtained from Shanghai Institute of Cell Biology (Shanghai, China). Cells were maintained in Dulbecco's Modified Eagle's medium (DMEM) with 10% fetal bovine serum (FBS; both from Beijing Solarbio Science & Technology Co., Ltd.), 100 U/ml penicillin and 100 μg/ml streptomycin at 37˚C with 5% CO_2. The medium was changed every three days.

At ~80% confluence, cells were harvested and a cell suspension with serum-free DMEM was prepared. The concentration of the cell suspension was $1x10^6$ cells/ml. Then, 1 ml of the cell suspension was added to each well of 6-well plates. miR-491-3p mimic (5'-CUUAUGCAAGAUUCCCUUCUAC-3'), mimic negative control (NC, 5'-GUAAUGCUAGAUUCGGUACUU G-3'), miR-491-3p inhibitor (5'-AGTAGAAGGGAATCT TGCATAAG-3'), and inhibitor NC (5'-ACAGAGCTATAG ATGTAAGTGAG-3') (Shanghai GenePharma Co., Ltd.) were transfected into A549 and H1299 cells according to the manufacturer's protocol using Lipofectamine® 2000 (Thermo Fisher Scientific, Inc.). pcDNA3.1-FGF5 plasmid and control vector (Shanghai Zeye Biotechnology, Co., Ltd.) were separately transfected into A549 cells similarly. Moreover, A549 cells were cotransfected with mimic NC and pcDNA3.1-FGF5 plasmid, or mimic NC and control vector, or miR-491-3p mimic and pcDNA3.1-FGF5 plasmid, or miR-491-3p mimic and control vector. The transfection was performed according to the manufacturer's protocol of Lipofectamine 2000. Cells were transfected for 8 h at 37˚C with 5% CO_2. Then, DMEM with 10% FBS was used to treat the cells for 48 h at 37˚C with 5% CO_2.

Cell counting kit-8 (CCK-8) assay. Cell viability was evaluated using a CCK-8 assay. A549 and H1299 cells were prepared into a cell suspension ($1x10^5$ cells/ml) with DMEM containing 10% FBS. The cell suspension (100 μl) was added to a 96-well plate for culturing at 37˚C with 5% CO_2. Cell viability was observed every 24 h. CCK-8 solution (10 μl) was added into each well and incubated for 2 h at 37˚C. The optical density (OD) was measured at 450 nm using a microplate reader (BioTek Instruments, Inc.).

Ethynyldeoxyuridine (EdU) experiment. cell proliferation was observed using the Edu experiment. The suspension ($1x10^4$ cells/ml, 1 ml) of A549 and H1299 cells was seeded in a 6-well plate and cultured at 37˚C with 5% CO_2 for 48 h. Subsequently, cell proliferation was observed using the EdU detection kit (Guangzhou Ribobio Co., Ltd.) according to the manufacturer instructions. Cells were stained using an anti-EdU working solution (100 μl, for 2 h at 37˚C) and 4'6-diamidino-2-phenylindole (DAPI, 1 mg/ml) was used to stain the nucleus (15 min at room temperature). Cells were observed and images were captured under a confocal laser scanning microscope (Olympus Corporation). The Edu staining positive cells (red fluorescent) and DAPI staining positive cells (blue fluorescence) were calculated using ImageJ software (Version 1.45s; National Institutes of Health). Five randomly-selected fields were observed in each group.

Matrigel experiment. The upper chamber (8-μm pore size) was precoated with Matrigel (30 min at 37˚C), followed by seeding with $2x10^4$ cells (dispersed in 200 μl serum-free DMEM). DMEM containing 10% FBS (600 μl) was added into the lower chamber. Cells were cultured for 24 h at 37˚C with 5% CO_2. Cells on the upper surface were gently scraped off using a cotton swab. Paraformaldehyde (4%) was used to fix (15 min at room temperature) the cells on the lower surface. Then, the invasive cells were stained with 0.1% crystal violet for 20 min at room temperature. The invasive cells in five randomly-selected fields were counted under a confocal microscope (Olympus Corporation).

Wound healing assay. A549 and H1299 cells were prepared into cell suspension with DMEM without FBS. The suspensions ($1x10^6$ cells/ml, 1 ml) were seeded onto a 6-well plate and incubated at 37˚C with 5% CO_2. When the cells attached to the bottom of the wells, they were scratched using a 100-μl sterile pipette tip. The initial wound width was measured and recorded. the residual liquid was replaced with fresh DMEM (without FBS). Cells were cultured at 37˚C with 5% CO_2. After 24 h, the final wound width was measured. The relative wound width was calculated (final wound width/the initial wound width).

Flow cytometric analysis. A549 and H1299 cells ($1x10^6$ cells/ml) were added into flow tubes. The cells were washed in pre-cooled phosphate buffer solution (PBS) three times. Then, they were washed in 1X binding buffer once. apoptosis (early + late) was detected using the Annexin V- fluorescein isothiocyanate apoptosis detection kit (Biovision, Inc.) according to the manufacturer's protocol. The percentage of apoptosis in cells was evaluated using flow cytometry (FACScan; BD Biosciences) and analyzed by the Diva software (version 8.0, Becton, Dickinson and Company).

Dual-luciferase reporter gene assay. Using TargetScan version 7.1. (http://www.targetscan.org/vert_71/), it was observed that FGF5 and miR-491-3p had common binding site in the 3'-UTR region. Based on this, dual-luciferase reporter gene assay was performed with A549 and H1299 cells to establish a relationship between miR-491-3p and FGF5. The cells ($1x10^5$ cells/ml) were seeded in a 6-well plate with serum-free DMEM. They were transfected with miR-491-3p mimic, mimic NC, miR-491-3p inhibitor, and inhibitor NC. Using Lipofectamine 2000, pmirGLO-FGF5-wild-type (WT) and pmirGLO-FGF5-mutant type (MUT) luciferase reporter vectors (Shanghai GenePharma Co., Ltd.) were individually transfected into A549 and H1299 cells. After incubating for 48 h at 37˚C, the luciferase activity was measured using the dual-luciferase reporter assay system (Promega Corporation). *Renilla* luciferase activity was used as control.

In vivo study. Animal experiments were approved (approval no. AE041A) by the Animal Ethics Committee of First Affiliated Hospital of Wannan Medical College Yijishan Hospital (Wuhu, China). The document of the Animal Ethics Committee was related to the animal experiments of the present study. A total of 12 BALB/c nude mice (male, 4 weeks old, weight 220-240 g, obtained from Vital River Laboratory Animal Technology; Beijing, China) were randomly divided into two groups: NC group (n=6) and miR-491-3p group (n=6). Lentiviruses (hU6-MCS-CMV-Puromycin) were purchased from Shanghai GeneChem Co., Ltd. The 293T cells were seeded at a density of $6x10^6$ cells/ml in a 15-cm culture dish, cultured at 37˚C with 5% CO_2 to 70-80% confluence, and the lentivirus plasmids were co-transfected into 293T cells using Lipofectamine® 2000 (Invitrogen; Thermo Fisher Scientific, Inc.), at 37˚C for 6 h. The supernatant of 293T cells transfected for 72 h was collected, centrifuged at 4,000 x g for 10 min at 4˚C to remove cell debris, filtered, centrifuged at 7,000 x g for 5 min at 4˚C, resuspended in ice-cold PBS to detect the titer, and stored at- 80˚C. Based on the transfection, the cells were divided into miR-491-3p and NC groups. The A549 cells at a density of $6x10^5$ cells/well in a six-well culture plate were infected with the miR-491-3p with a multiplicity of infection of 20, and the miR-491-3p gene expression sequence carried by the lentivirus was integrated into the cell to obtain stable overexpression. A549 cells were transfected with lentivirus/medium at a ratio of 1:50. Stable cell lines were selected by puromycin (Sigma-Aldrich; Merck KGaA) at 5 μg/ml for 2 weeks. The lentiviral vectors contained enhanced green fluorescent protein (eGFP). Lentiviral-transfected A549 cells were harvested and dispersed into PBS to prepare cell suspension. The density of each cell suspension samples was $1x10^7$ cells/ml. Nude mice of NC group and miR-491-3p group were injected subcutaneously with 100 μl of the corresponding cell suspension samples. The injection site was on the back. After injection, nude mice were kept at 22±2˚C for 28 days in a 12 h day/night cycle room with free access to food and water. The tumor volume was measured at 7-day intervals by (length x width^2)/2. Nude mice were then euthanized by rapid cervical dislocation after deep anesthesia with 5% isoflurane. The xenograft tumor tissues were collected, weighted and stored in a refrigerator at -80˚C. During the 28-day, the humane endpoint of mice was defined as the following symptoms: hunched posture, pale extremities, inactivity and dyspnea; and the tumor size exceeded 20 mm in one dimension. Mice with these aforementioned symptoms were then immediately euthanized. The regularly tumor progression was checked every day by using vernier caliper in order to ensure the tumor size was within the allowable range of humane endpoints.

Immunohistochemistry (IHC). The protein expression of FGF5 and Ki67 in the xenograft tumor tissues was detected by performing IHC. Briefly, the xenograft tumor tissues were embedded into paraffin before being cut into 4-μm sections. After dewaxing in xylene and rehydration in descending ethanol series, the sections were treated with 3% H_2O_2 for 10 min at room temperature and then subjected to antigen retrieval in boiled citrate buffer. The blockage of the sections was implemented by 5% normal goat serum. Thereafter, the sections were incubated overnight with rabbit anti-FGF5 primary antibody (1:100; cat. no. ab88118) and rabbit anti-Ki67 primary antibody (1:100; cat. no. ab15580; both from Abcam) at 4˚C. PBS was utilized to wash the sections twice. The sections were then treated for 30 min with horseradish peroxidase-conjugated goat anti-rabbit secondary antibody (1:200; cat. no. ab6721; Abcam) at 37˚C. Post twice washing with PBS, the sections were stained with 3,3'-diaminobenzidine (for 5 min at room temperature) and hematoxylin (for 30 sec at room temperature). After dehydration, the sections were sealed in neutral resin and observed under a light microscope (Olympus Corporation; magnification, x200; scale bar: 100 μm).

Reverse transcription-quantitative polymerase chain reaction (RT-qPCR). TRIzol® reagent (Wuhan Boster Biological Technology, Ltd.) was added into tissues and cells to extract total RNA. The total RNA sample was reverse transcribed to obtain the cDNA template. It was reverse transcribed using the PrimeScript RT Master Mix (Takara Bio, Inc.) according to the manufacturer's protocol. RT-qPCR was performed using the SYBR Premix Ex Taq (Takara Bio, Inc.) in an ABI 7500 Real-Time PCR system (Applied Biosystems; Thermo Fisher Scientific, Inc.). The thermocycling conditions were as follows: 40 cycles at 95˚C for 5 min, 95˚C for 30 sec, 60˚C for 45 sec, and 72˚C for 30 min. The primers were designed by Shanghai GenePharma Co., Ltd. and the sequences were as follows: miR-491-3p forward, 5'-AGTGGGGAACCCTTCC-3' and reverse, 5'-GAACATGTCTGCG-TATCTC-3'; U6 forward, 5'-AAAGCAAATCATCGGACGACC-3' and reverse, 5'-GTA CAACACATTGTTTCCTCGGA-3'; FGF5 forward, 5'-TTC TCTTTCACAGCACCAAA-3' and reverse, 5'-CTCCTTGCT TCTAACCCATC-3'; and β-actin forward, 5'-AGCGAGCAT CCCCCAAAGTT-3' and reverse, 5'-GGGCACGAAGGC

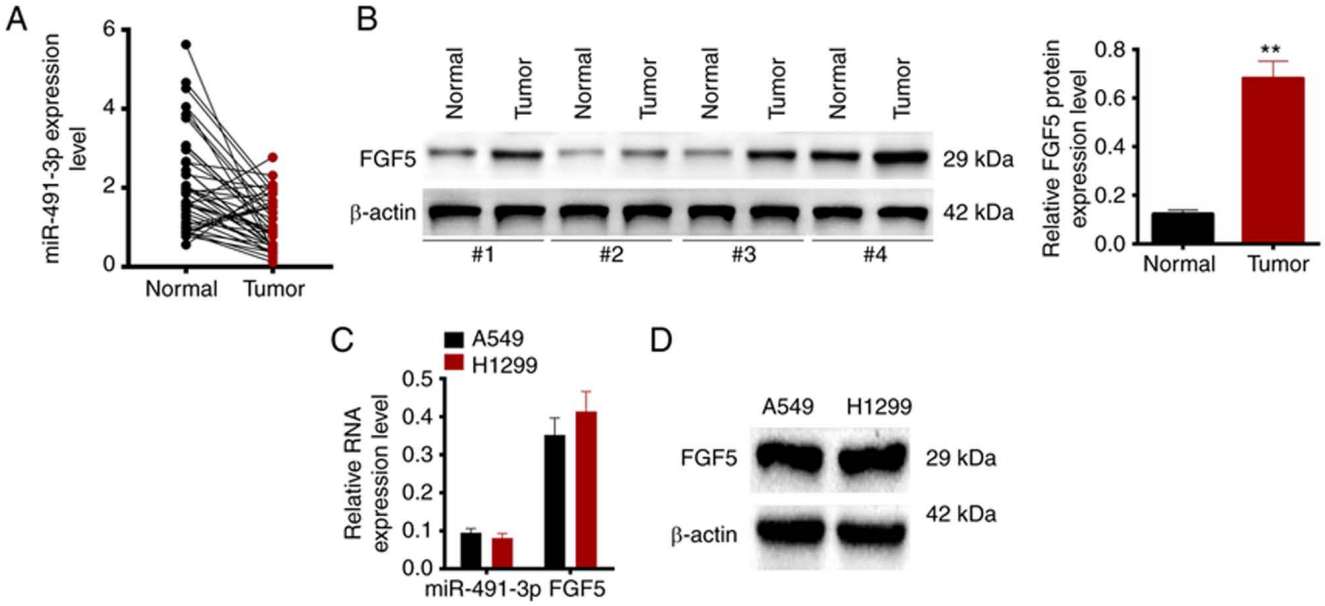

Figure 1. miR-491-3p is upregulated and FGF5 is downregulated in NSCLC tissues. (A) RT-qPCR revealed that miR-491-3p was upregulated in the tumor tissues of patients with NSCLC. (B) Western blot analysis indicated that FGF5 protein was downregulated in tumor tissues of patients with NSCLC. (C) miR-491-3p and FGF5 mRNA expression in NSCLC cells was monitored by RT-qPCR. (D) FGF5 protein expression detection in NSCLC cells was implemented by western blot analysis. **P<0.01. miR, microRNA; FGF5, fibroblast growth factor 5; NSCLC, non-small cell lung cancer; RT-qPCR, reverse transcription-quantitative PCR.

TCATCATT-3'. U6 was used as control for miR-491-3p relative expression using the $2^{-\Delta\Delta Cq}$ method (19).

Western blot analysis. Total proteins were extracted from tissues and cells using RIPA lysis buffer (Beyotime Institute of Biotechnology) containing protease inhibitor. The concentration of total proteins was determined using a BCA kit (Beyotime Institute of Biotechnology). A 10 μg protein sample was mixed with 1X loading buffer and separated using 10% sodium dodecyl sulfate-polyacrylamide gel electrophoresis. the proteins were transferred onto a polyvinylidene fluoride (PVDF) membrane and blocked with 5% skimmed milk for 1 h at room temperature. Rabbit anti-FGF5 primary antibody (1:1,000) and rabbit anti-β-actin primary antibody (1:1,000; cat. no. ab8227; Abcam) were used to probe the PVDF membrane for 12 h at 4˚C. horseradish peroxidase-conjugated goat anti-rabbit secondary antibody (1:2,000) was used to treat the PVDF membrane for 1 h at room temperature. The protein blots were visualized using enhanced chemiluminescence detection reagent (Beyotime Institute of Biotechnology). The quantitative analysis of proteins was performed using Quantity one software (version 4.6.3; Bio-Rad Laboratories, Inc.). β-actin was used as the control for the relative expression of FGF5 protein.

Statistical analysis. All experiments were performed in triplicate. SPSS 19.0 (IBM Corp.) and GraphPad Prism 5.0 software (GraphPad Software, Inc.) were used to analyze the data (mean ± standard deviation). The two-tailed paired Student's t-test was used for the comparison between two groups. more than two groups were compared using One-way ANOVA followed by Tukey's post hoc test. Pearson's correlation coefficient test was employed to identify the correlation between miR-491-3p and FGF5 mRNA in tumor tissues of patients with NSCLC. P<0.05 was considered to indicate a statistically significant difference.

Results

miR-491-3p is downregulated and FGF5 is upregulated in patients with NSCLC. In the present study, the expression of miR-491-3p and FGF5 protein was evaluated in 43 patients with NSCLC. miR-491-3p expression was distinctly low in tumor tissues compared with the adjacent normal tissues (P<0.01) (Fig. 1A). By contrast, FGF5 protein expression was higher in tumor tissues of patients with NSCLC compared with normal adjacent tissues (P<0.01) (Fig. 1B). The relationship between miR-491-3p expression and clinicopathological characteristics of patients was demonstrated in Table I. NSCLC patients with low miR-491-3p expression exhibited advanced tumor stages and lymphatic metastasis (P<0.05). Additionally, the relationship between FGF5 mRNA expression and clinicopathological characteristics of NSCLC patients was listed in Table II. High FGF5 mRNA expression was associated with advanced TNM stage and lymphatic metastasis of NSCLC patients (P<0.05). Therefore, miR-491-3p was downregulated and FGF5 was upregulated in tumor tissues of NSCLC patients. Low miR-491-3p expression and high FGF5 mRNA expression was associated with poor outcomes in NSCLC patients, including advanced TNM stage and lymph node metastasis.

Additionally, the expression of miR-491-3p, FGF5 mRNA and protein expression in A549 and H1299 cells were monitored by RT-qPCR and western blotting (Fig. 1C and D). An opposite trend was found between miR-491-3p and FGF5 expression levels in A549 and H1299 cells.

miR-491-3p overexpression inhibits viability, proliferation, migration and invasion, and promotes apoptosis in NSCLC cells. A549 and H1299 cells were transfected with miR-491-3p mimic and corresponding NC. After transfection, cell viability and proliferation were investigated using CCK-8 assay and Edu

Table I. The relationship between miR-491-3p expression and clinicopathological characteristics of patients with non-small cell lung cancer.

Clinicopathological characteristics	Number of patients	Expression level of miR-491-3p		P-value
		Low (<median)	High (≥ median)	
Number	43	21	22	
Age, years				0.625
<60	18	8	10	
≥60	25	13	12	
Sex				0.658
Female	19	10	9	
Male	24	11	13	
TNM stage				0.004
I/II	20	5	15	
III/IV	23	16	7	
Pathological type				0.745
Squamous	22	12	10	
Adenocarcinoma	14	6	8	
Large cell lung cancer	7	3	4	
Smoking status				0.850
Non-smoker	17	8	9	
Smoker	26	13	13	
Lymphatic Metastasis				0.002
No	16	3	13	
Yes	27	18	9	

miR, microRNA.

experiment, respectively. After 48 h, the OD (at 450 nm) values for A549 and H1299 cells in the miR-491-3p mimic group were significantly lower compared with the NC mimic group (P<0.05 or P<0.01; Fig. 2A). in the miR-491-3p mimic group, the number of Edu positive cells was decreased compared with the NC mimic group (P<0.01; Fig. 2B). Therefore, miR-491-3p overexpression inhibited viability and proliferation of NSCLC cells.

The Matrigel experiment was used to study the invasion ability of the NSCLC cells. As revealed in Fig. 2C, compared with the NC mimic group, A549 and H1299 cells of the miR-491-3p mimic group exhibited a significantly lower invasive cell number (P<0.01). Wound healing assay demonstrated a significantly higher relative wound width in A549 and H1299 cells of the miR-491-3p mimic group compared with the NC mimic group (P<0.01; Fig. 2D). These data suggested that miR-491-3p overexpression inhibits invasion and migration of NSCLC cells.

Flow cytometric analysis was utilized for observing cell apoptosis. The percentage of apoptosis was subsequently investigated. A549 and H1299 cells in the miR-491-3p mimic group showed a higher cell apoptotic percentage, compared with the NC mimic group (P<0.01; Fig. 2E). Therefore, miR-491-3p overexpression facilitated apoptosis in NSCLC cells.

miR-491-3p directly inhibits the expression of FGF5. Using TargetScan 7.1. online prediction software, it was identified that FGF5 possessed a binding site for miR-491-3p in the 3'-UTR region (Fig. 3A). Subsequently, the dual-luciferase reporter gene assay was used to detect the relationship between miR-491-3p and FGF5. As revealed in Fig. 3B, the relative luciferase activity of WT-FGF5 reporter in A549 and H1299 cells was lower in the miR-491-3p mimic group compared with the NC mimic group (P<0.01). By contrast, the miR-491-3p inhibitor group revealed higher relative luciferase activity of WT-FGF5 reporter in A549 and H1299 cells compared with the NC inhibitor (P<0.01). However, no significant changes in relative luciferase activity of MUT-FGF5 reporter were observed among the four groups. The FGF5 mRNA expression in clinical samples of patients with NSCLC was monitored using RT-qPCR. Significantly upregulated FGF5 mRNA was detected in tumor tissues compared with that in adjacent normal tissues (P<0.01). The miR-491-3p and FGF5 mRNA level in tumor tissues of patients with NSCLC exhibited a negative correlation (P=0.0008; Fig. 3C). Additionally, FGF5 mRNA and protein expression was detected in A549 and H1299 cells of the four groups. As a result, the FGF5 mRNA and protein expression was decreased in A549 and H1299 cells of the miR-491-3p mimic group in comparison with the NC mimic group (P<0.01). Compared with the NC inhibitor group, FGF5 mRNA and protein expression significantly increased in A549 and H1299 cells of the miR-491-3p inhibitor group (P<0.01; Fig. 3D). These results indicated that FGF5 expression is directly inhibited by miR-491-3p.

Table II. The relationship between FGF5 expression and clinicopathological characteristics of patients with non-small cell lung cancer.

Clinicopathological characteristics	Number of patients	Expression level of FGF5		P-value
		Low (<median)	High (≥ median)	
Number	43	21	22	
Age, years				0.429
<60	18	8	10	
≥60	25	13	12	
Sex				0.227
Female	19	11	8	
Male	24	10	14	
TNM stage				0.04
I/II	20	14	6	
III/IV	23	7	16	
Pathological type				0.745
Squamous	22	10	12	
Adenocarcinoma	14	8	6	
Large cell lung cancer	7	3	4	
Smoking status				0.760
Non-smoker	17	10	7	
Smoker	26	11	15	
Lymphatic Metastasis				0.012
No	16	12	4	
Yes	27	9	16	

FGF5, fibroblast growth factor 5.

FGF5 upregulation reverses the inhibitory effects of miR-491-3p on NSCLC cell malignant phenotype. pcDNA3.1-FGF5 plasmid and control vectors were transfected into A549 cells. The transfection efficiency was analyzed using RT-qPCR. A549 cells of the FGF5 group exhibited significantly higher FGF5 protein expression compared with the vector group (P<0.01; Fig. 4A).

After 72 h, compared with the NC mimic + vector group, the OD value of A549 cells decreased in the miR-491-3p mimic + vector and increased in NC mimic + FGF5 groups, respectively (P<0.01). Meanwhile, compared with the miR-491-3p mimic + FGF5 group, the OD value of A549 cells in the miR-491-3p mimic + vector group decreased, and in the NC mimic + FGF5 group increased (P<0.01; Fig. 4B).

Compared with the NC mimic + vector group, the Edu positive cell number decreased in the miR-491-3p mimic + vector and increased in the NC mimic + FGF5 groups, respectively (P<0.01). Compared with the miR-491-3p mimic + FGF5 group, the Edu positive cell number decreased in the miR-491-3p mimic + vector group and increased in the NC mimic + FGF5 group, respectively (P<0.01; Fig. 4C).

In the Matrigel experiment, compared with the NC mimic + vector group the invasive cell numbers were lower in the miR-491-3p mimic + vector and higher in the NC mimic + FGF5 groups, respectively (P<0.01). Similarly, compared with the miR-491-3p mimic + FGF5 group, the invasive cell numbers decreased in the miR-491-3p mimic + vector and increased in the NC mimic + FGF5 groups, respectively (P<0.01; Fig. 4D).

Wound healing assay was performed to evaluate the cell migration ability. The results showed that compared with the NC mimic + vector group, the relative wound width was larger in the miR-491-3p mimic + vector and smaller in the NC mimic + FGF5 groups, respectively (P<0.01). Similarly, compared with the miR-491-3p mimic + FGF5 group, the relative wound width was larger in the miR-491-3p mimic + vector and smaller in the NC mimic + FGF5 groups, respectively (P<0.01; Fig. 4E).

Flow cytometric analysis was used to detect apoptosis. Compared with the NC mimic + vector group, the cell apoptosis percentage was higher in the miR-491-3p mimic + vector and lower in the NC mimic + FGF5 groups, respectively (P<0.01). Moreover, compared with the miR-491-3p mimic + FGF5 group, the cell apoptosis percentage of A549 cells was higher in the miR-491-3p mimic + vector and lower in the NC mimic + FGF5 groups, respectively (P<0.01; Fig. 4F). These results suggested that FGF5 upregulation reversed the inhibitory effect of miR-491-3p on the NSCLC cell malignant phenotype.

miR-491-3p overexpression suppresses the in vivo growth of NSCLC. In vivo study was performed to monitor the effect of miR-491-3p on the *in vivo* development of NSCLC. As revealed in Fig. 5A and B, miR-491-3p overexpression suppressed the

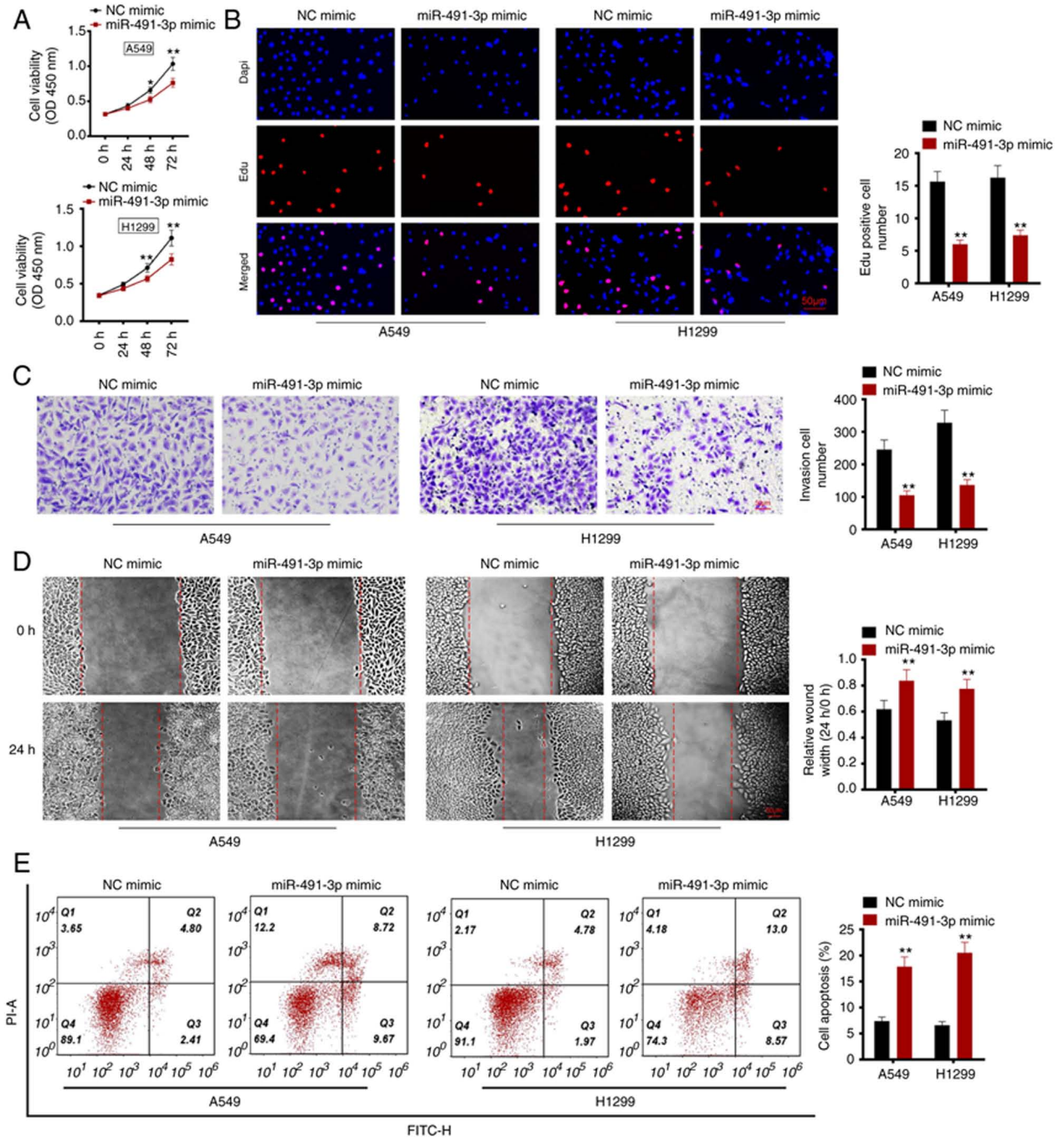

Figure 2. miR-491-3p overexpression inhibits viability, proliferation, migration and invasion, and promotes apoptosis in NSCLC cells. (A) Cell Counting Kit-8 assay illustrated that miR-491-3p overexpression inhibited NSCLC cell viability. (B) Edu experiment indicated that miR-491-3p overexpression inhibited NSCLC cell proliferation. 200x magnification. Scale bar: 50 μm. (C) Matrigel experiment indicated that miR-491-3p overexpression suppressed NSCLC cell invasion. 200x magnification. Scale bar: 50 μm. (D) Wound healing assay revealed that miR-491-3p overexpression suppressed NSCLC cell migration. (E) Flow cytometry was used to measure cell apoptosis. miR-491-3p overexpression promoted NSCLC cell apoptosis. *P<0.05 and **P<0.01. miR, microRNA; NSCLC, non-small cell lung cancer; NC, negative control.

in vivo growth of NSCLC cells, as proved by the lower tumor volume and weight in miR-491-3p group compared with the NC group (P<0.01). Xenograft tumor tissues were subjected to RT-qPCR to detect the expression of miR-491-3p and FGF5 mRNA. As a result, higher miR-491-3p expression as well as lower FGF5 mRNA expression was revealed in the xenograft tumor tissues of miR-491-3p group when compared with NC group (P<0.01; Fig. 5C). Simultaneously, less Ki67 and FGF5 protein expression was identified in the xenograft tumor tissues of miR-491-3p group compared with the NC group (Fig. 5D). Thus, miR-491-3p suppressed the *in vivo* growth of NSCLC.

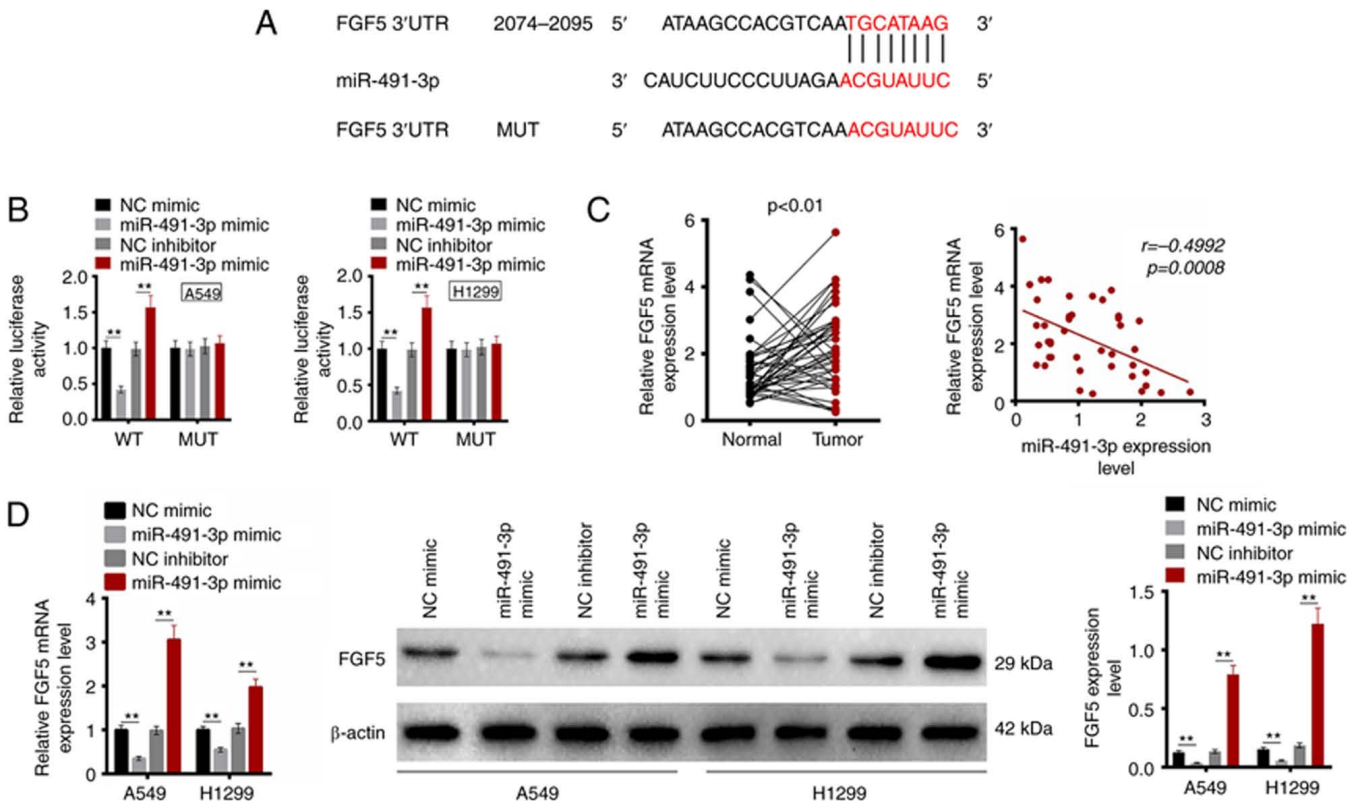

Figure 3. miR-491-3p directly inhibits the expression of FGF5. (A) TargetScan 7.1 online prediction software revealed that FGF5 possessed a binding site for miR-491-3p in the 3'-UTR region. (B) Dual luciferase reporter gene assay verified that FGF5 is a target gene of miR-491-3p. (C) FGF5 mRNA expression in clinical samples of patients with NSCLC was detected by RT-qPCR. Pearson's correlation coefficient analysis was employed to identify the correlation between miR-491-3p and FGF5 mRNA in tumor tissues of patients NSCLC. (D) RT-qPCR and western blotting indicated that miR-491-3p suppressed the expression of FGF5 mRNA and protein. **P<0.01. miR, microRNA; FGF5, fibroblast growth factor 5; UTR, untranslated; RT-qPCR, reverse transcription-quantitative PCR; WT, wild-type; MUT, mutant; NC, negative control.

Discussion

The expression of miRNA is tissue-specific and is usually dysregulated in multiple human types of cancer (20). In the present study, the tumor-suppressive role of miR-491-3p was demonstrated in NSCLC. Low miR-491-3p expression was associated with poor outcomes in patients with NSCLC, including advanced TNM stage as well as lymph node metastasis. The overexpression of miR-491-3p promoted apoptosis and inhibited viability, proliferation, migration and invasion of the NSCLC cells. Additionally, miR-491-3p overexpression suppressed the *in vivo* growth of NSCLC. This is the first time, to the best of our knowledge, that miR-491-3p is identified as a tumor suppressor in NSCLC.

miRNAs are important regulators of tumorigenesis. They can promote degradation in mRNA or suppress translation of proteins by interacting with the 3'-UTR region of the mRNA of target genes (21). In recent years, the role of miRNAs in the progression of NSCLC has attracted extensive attention. For instance, miR-605-5p was revealed to be overexpressed in NSCLC. The malignant phenotype of NSCLC cells, such as migration and invasion, were intensified after the overexpression of miR-605-5p (22). miR-512-5p played a tumor-suppressive effect on NSCLC. The upregulation of miR-512-5p enhanced the apoptosis and suppressed the invasion of NSCLC cells (23). By contrast, miR-148b was identified to be poorly expressed in NSCLC. NSCLC patients with low miR-148b expression showed shorter overall survival. The elevated miR-148b expression suppressed NSCLC cell growth, migration and invasion (24). The decreased miR-654-3p expression was associated with node metastasis in NSCLC. NSCLC cells with overexpressed miR-654-3p possessed the attenuated proliferation ability and the enhanced apoptotic capacity (25). Heretofore, the function of miR-491-3p in NSCLC has never been explored. Previous studies have identified that miR-491-3p exerted the tumor suppressor role in human malignant tumors, such as hepatocellular carcinoma and osteosarcoma (13,14). Similarly, the tumor-suppressing function of miR-491-3p in NSCLC was confirmed in the present study. the present study was the first to identify the tumor suppressor function of miR-491-3p in NSCLC by directly targeting and inhibiting FGF5. In clinical practice, the effective delivery of miRNAs to the tumor sites remains an important challenge in the transition of miRNAs therapy. Notably, recently, it has been demonstrated that nano-formulations of miRNAs not only reduce systemic and cytotoxicity, but also elevate the bioavailability of miRNAs and the accumulation of miRNAs at the tumor site (26). Therefore, in the future, the development of nano-formulations of miR-491-3p for NSCLC target therapy will be a promising direction to realize the clinical use of miR-491-3p.

FGF5 is involved in multiple biological processes, such as tissue growth and repair (27). A recent study has proved that

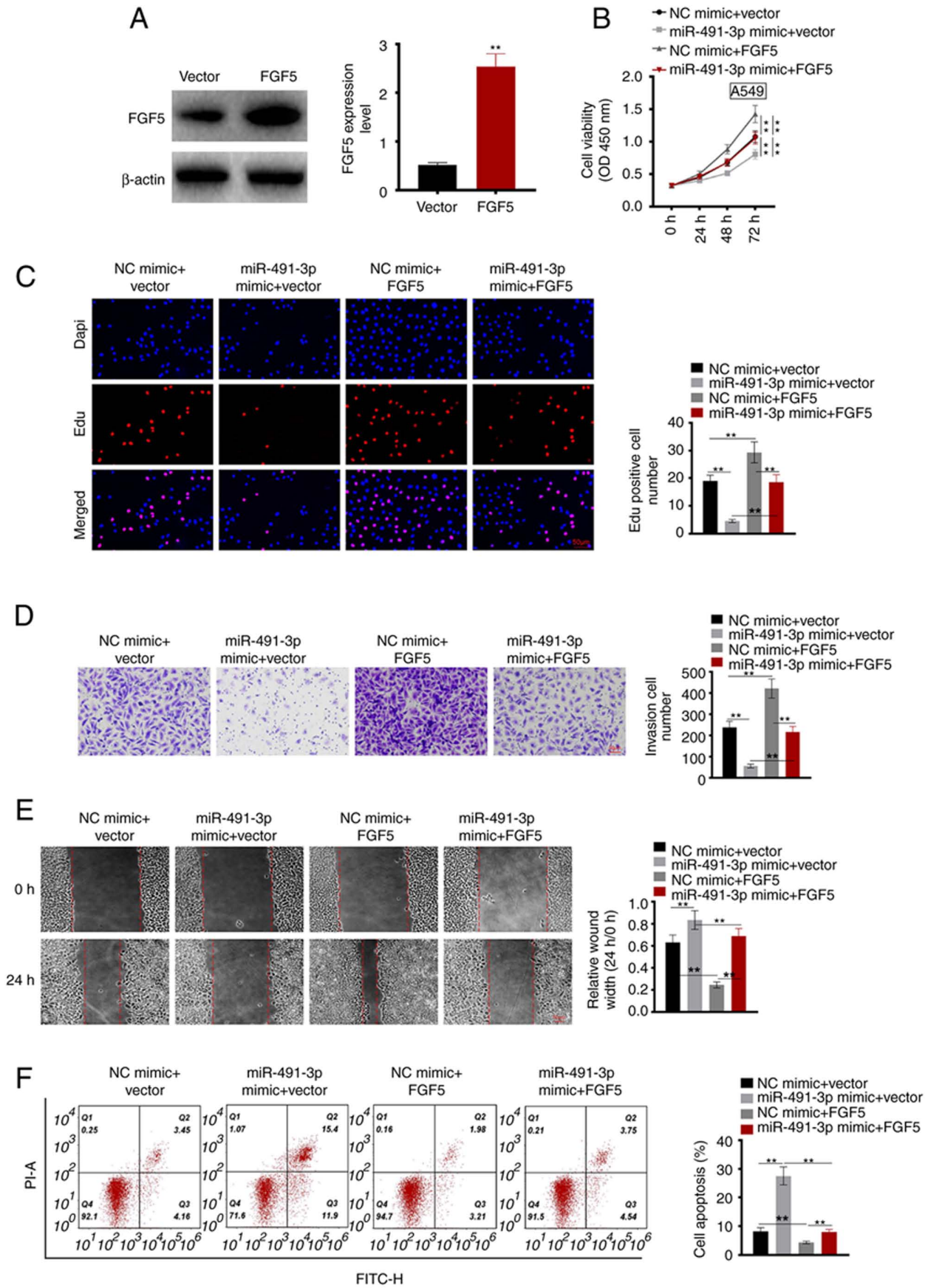

Figure 4. FGF5 upregulation reverses the inhibitory effects of miR-491-3p on NSCLC cell malignant phenotype. (A) A549 cells were successfully transfected using pcDNA3.1-FGF5 plasmid and control vector. (B) FGF5 upregulation reversed the inhibitory effects of miR-491-3p on NSCLC cell viability. (C) FGF5 upregulation reversed the inhibitory effects of miR-491-3p on NSCLC cell proliferation. 200x magnification. Scale bar: 50 μm. (D) FGF5 upregulation reversed the inhibitory effects of miR-491-3p on NSCLC cell invasion. 200x magnification. Scale bar: 50 μm. (E) FGF5 upregulation reversed the inhibitory effects of miR-491-3p on NSCLC cell migration. (F) FGF5 upregulation reversed the effects of miR-491-3p on NSCLC cell apoptosis. **P<0.01. FGF5, fibroblast growth factor 5; miR, microRNA; NSCLC, non-small cell lung cancer; NC, negative control.

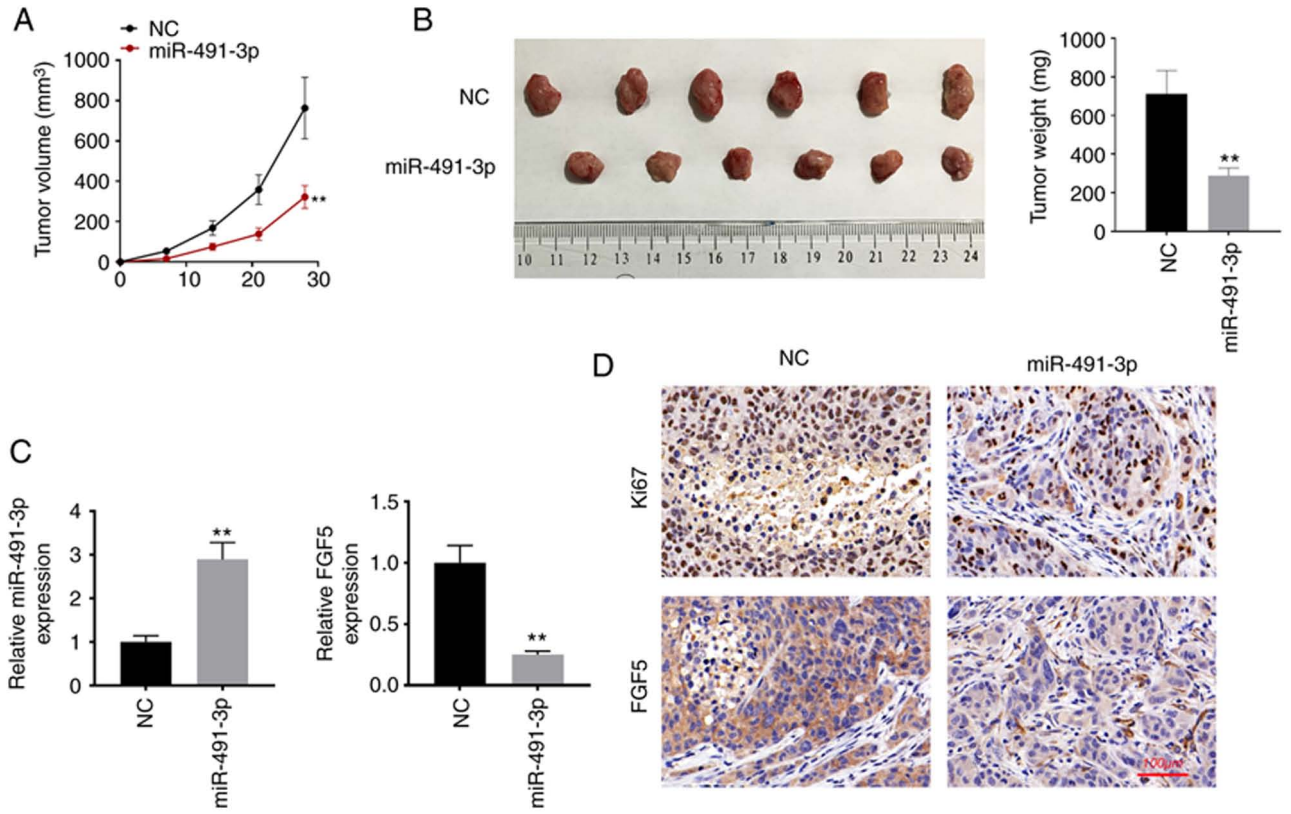

Figure 5. miR-491-3p overexpression suppresses the *in vivo* growth of NSCLC. (A and B) The volume and weight of xenograft tumor tissues was measured. (C) Reverse transcription-quantitative PCR was implemented to detect the expression of miR-491-3p and FGF5 mRNA in xenograft tumor tissues. (D) Immunohistochemical analysis was carried out to detect the expression of Ki67 and FGF5 protein in xenograft tumor tissues. 200x magnification. Scale bar: 100 μm. **P<0.01. miR, microRNA; NSCLC, non-small cell lung cancer; FGF5, fibroblast growth factor 5; NC, negative control.

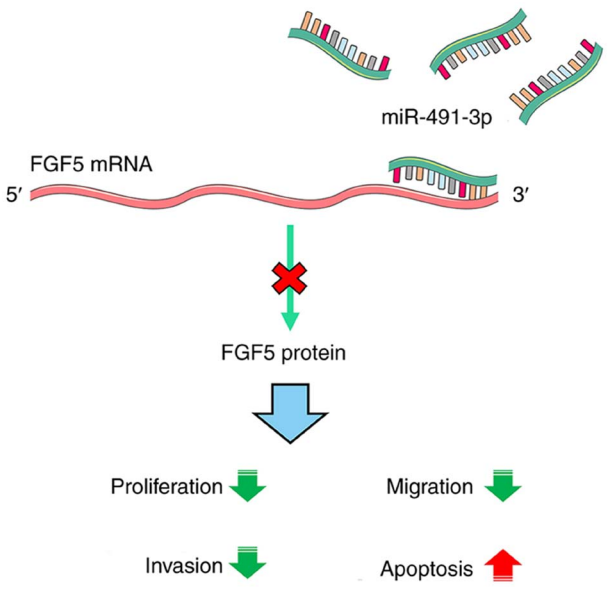

Figure 6. Mechanism diagram of the present study.

FGF5 is a cancer promoting factor. FGF5 upregulation in breast cancer was associated with poor prognosis (28). Han *et al* (29) reported that FGF5 was required for the proliferation of osteosarcoma cells. The addition of exogenous FGF5 enhanced proliferation and suppressed apoptosis in osteosarcoma cells by activating the mitogen-activated protein kinase (MAPK) signaling pathway. the upregulation of FGF5 partially reverses the suppression of miR-567 in osteosarcoma cell migration and invasion (30). Moreover, FGF5 was verified to be a target of miR-188-5p. restoring FGF5 expression reversed the inhibition effect of miR-188-5p on the metastasis of hepatocellular carcinoma (31). FGF5 expression is aberrantly elevated in pancreatic cancer. The growth of pancreatic cancer cells is significantly exacerbated after treatment with exogenous FGF5. However, the addition of exogenous FGF5 enhanced the activity of the MAPK signaling pathway (32). Similarly, it was demonstrated that FGF5 was highly expressed in patients with NSCLC. miR-491-3p directly restrained the expression of FGF5. Moreover, restoring the FGF5 expression abrogated the inhibition of miR-491-3p on the malignant phenotype of NSCLC cells. Thus, miR-491-3p could suppress the progression of NSCLC by targeting FGF5. The mechanism diagram is revealed in Fig. 6.

Nevertheless, there are certain limitations to the present study. First, the sample size/power analysis was not performed. Moreover, a previous study has reported that FGF5 could promote the activity of the MAPK signaling pathway (29). However, due to laboratory limitations, it could not be confirmed whether FGF5 promoted NSCLC progression via regulating the MAPK signaling pathway activity. Furthermore, the present study focused on miR-491-3p and its downstream gene in NSCLC. It should be better to explore whether miR-491-3p expression correlates with driver gene status. Meanwhile, the concomitant mutations or co-mutations

should also be investigated. These aforementioned issues will be addressed in future studies.

These findings indicated that miR-491-3p acts as a tumor suppressor in NSCLC. It weakens the proliferation, migration, invasion, and enhances the apoptosis of NSCLC cells by targeting FGF5. restoring FGF5 expression reverses the suppression role of miR-491-3p on the NSCLC cell malignant phenotype. More importantly, miR-491-3p overexpression suppresses the *in vivo* growth of NSCLC. Therefore, miR-491-3p may be a potential target for the treatment of NSCLC.

Acknowledgements

Not applicable.

Funding

No funding was received.

Availability of data and materials

All data generated or analyzed during this study are included in this published article.

Authors' contributions

GZ was responsible for study design and data collection. LW contributed to data analysis. GZ and HZ were in charge of clinical data recording and data analysis. GZ, HZ and LW performed the experiments. GZ, HZ and LW wrote the manuscript. All authors read and approved the final manuscript. GZ and LW confirm the authenticity of all the raw data.

Ethics approval and consent to participate

The research protocol was reviewed and approved (approval no. TCH036) by the Ethics Committee of the First Affiliated Hospital of Wannan Medical College Yijishan Hospital (Wuhu, China) and was in line with the Declaration of Helsinki. Animal experiments were approved (approval no. AE041A) by the Animal Ethics Committee of First Affiliated Hospital of Wannan Medical College Yijishan Hospital (Wuhu, China). Written informed consent was obtained from all patients.

Patient consent for publication

Not applicable.

Competing interests

The authors declare that they have no competing interests.

References

1. Khanmohammadi A, Aghaie A, Vahedi E, Qazvini A, Ghanei M, Afkhami A, Hajian A and Bagheri H: Electrochemical biosensors for the detection of lung cancer biomarkers: A review. Talanta 206: 120251, 2020.
2. Yu Q, Xu L, Chen L, Sun B, Yang Z, Lu K and Yang Z: Vinculin expression in non-small cell lung cancer. J Int Med Res 48: 300060519839523, 2020.
3. Gelatti AC, Drilon A and Santini FC: Optimizing the sequencing of tyrosine kinase inhibitors (TKIs) in epidermal growth factor receptor (EGFR) mutation-positive non-small cell lung cancer (NSCLC). Lung Cancer 137: 113-122, 2019.
4. Brozos-Vázquez EM, Díaz-Peña R, García-González J, León-Mateos L, Mondelo-Macía P, Peña-Chilet M and López-López R: Immunotherapy in nonsmall-cell lung cancer: Current status and future prospects for liquid biopsy. Cancer Immunol Immunother 70: 1177-1188, 2021.
5. Alexander M, Kim SY and Cheng H: Update 2020: Management of non-small cell lung cancer. Lung 198: 897-907, 2020.
6. Chen X, Zhao L, Kang Y, He Z, Xiong F, Ling X and Wu J: Significant suppression of non-small-cell lung cancer by hydrophobic poly(ester amide) nanoparticles with high docetaxel loading. Front Pharmacol 9: 118, 2018.
7. Zhong W, Zhang X, Zeng Y, Lin D and Wu J: Recent applications and strategies in nanotechnology for lung diseases. Nano Res 14: 2067-2089, 2021.
8. Xiong F, Ling X, Chen X, Chen J, Tan J, Cao W, Ge L, Ma M and Wu J: Pursuing specific chemotherapy of orthotopic breast cancer with lung metastasis from docking nanoparticles driven by bioinspired exosomes. Nano Lett 19: 3256-3266, 2019.
9. Naeli P, Yousefi F, Ghasemi Y, Savardashtaki A and Mirzaei H: The role of MicroRNAs in lung cancer: Implications for diagnosis and therapy. Curr Mol Med 20: 90-101, 2020.
10. Grossi I, Salvi A, Abeni E, Marchina E and De Petro G: Biological function of microRNA193a-3p in health and disease. Int J Genomics 2017: 5913195, 2017.
11. Shan C, Chen X, Cai H, Hao X, Li J, Zhang Y, Gao J, Zhou Z, Li X, Liu C, *et al*: The emerging roles of autophagy-related MicroRNAs in cancer. Int J Biol Sci 17: 134-150, 2021.
12. Hu Y, Zhao M, Li L, Ding J, Gui YM and Wei TW: miR-491-3p is downregulated in retinoblastoma and inhibit tumor cells growth and metastasis by targeting SNN. Biochem Genet 59: 453-474, 2021.
13. Duan J, Liu J, Liu Y, Huang B and Rao L: miR-491-3p suppresses the growth and invasion of osteosarcoma cells by targeting TSPAN1. Mol Med Rep 16: 5568-5574, 2017.
14. Zhao Y, Qi X, Chen J, Wei W, Yu C, Yan H, Pu M, Li Y, Miao L, Li C and Ren J: The miR-491-3p/Sp3/ABCB1 axis attenuates multidrug resistance of hepatocellular carcinoma. Cancer Lett 408: 102-111, 2017.
15. Zheng G, Jia X, Peng C, Deng Y, Yin J, Zhang Z, Li N, Deng M, Liu X, Liu H, *et al*: The miR-491-3p/mTORC2/FOXO1 regulatory loop modulates chemo-sensitivity in human tongue cancer. Oncotarget 6: 6931-6943, 2015.
16. Wang X, He Y, Mackowiak B and Gao B: MicroRNAs as regulators, biomarkers and therapeutic targets in liver diseases. Gut 70: 784-795, 2021.
17. Zhou Y, Yu Q, Chu Y, Zhu X, Deng J, Liu Q and Wang Q: Downregulation of fibroblast growth factor 5 inhibits cell growth and invasion of human nonsmall-cell lung cancer cells. J Cell Biochem: Dec 5, 2018 (Epub ahead of print). doi: 10.1002/jcb.28107.
18. Zhao T, Qian K and Zhang Y: High expression of FGF5 is an independent prognostic factor for poor overall survival and relapse-free survival in lung adenocarcinoma. J Comput Biol 27: 948-957, 2020.
19. Livak KJ and Schmittgen TD: Analysis of relative gene expression data using real-time quantitative PCR and the 2(-Delta Delta C(T)) method. Methods 25: 402-408, 2001.
20. Liang G, Meng W, Huang X, Zhu W, Yin C, Wang C, Fassan M, Yu Y, Kudo M, Xiao S, *et al*: miR-196b-5p-mediated downregulation of TSPAN12 and GATA6 promotes tumor progression in non-small cell lung cancer. Proc Natl Acad Sci USA 117: 4347-4357, 2020.
21. Correia de Sousa M, Gjorgjieva M, Dolicka D, Sobolewski C and Foti M: Deciphering miRNAs' action through miRNA editing. Int J Mol Sci 20: 6249, 2019.
22. Liao Y, Cao L, Wang F and Pang R: miR-605-5p promotes invasion and proliferation by targeting TNFAIP3 in non-small-cell lung cancer. J Cell Biochem 121: 779-787, 2020.
23. Wang Z, Zhu X, Zhang T and Yao F: miR-512-5p suppresses the progression of non-small cell lung cancer by targeting β-catenin. Oncol Lett 19: 415-423, 2020.
24. Jiang Z, Zhang J, Chen F and Sun Y: miR-148b suppressed non-small cell lung cancer progression via inhibiting ALCAM through the NF-κB signaling pathway. Thorac Cancer 11: 415-425, 2020.

25. Pu JT, Hu Z, Zhang DG, Zhang T, He KM and Dai TY: miR-654-3p suppresses non-small cell lung cancer tumourigenesis by inhibiting PLK4. Onco Targets Ther 13: 7997-8008, 2020.
26. Ganju A, Khan S, Hafeez BB, Behrman SW, Yallapu MM, Chauhan SC and Jaggi M: miRNA nanotherapeutics for cancer. Drug Discov Today 22: 424-432, 2017.
27. Kehler JS, David VA, Schäffer AA, Bajema K, Eizirik E, Ryugo DK, Hannah SS, O'Brien SJ and Menotti-Raymond M: Four independent mutations in the feline fibroblast growth factor 5 gene determine the long-haired phenotype in domestic cats. J Hered 98: 555-566, 2007.
28. Huang Y, Wang Y and Yang Y: Expression of fibroblast growth factor 5 (FGF5) and its influence on survival of breast cancer patients. Med Sci Monit 24: 3524-3530, 2018.
29. Han D, Wang M, Yu Z, Yin L, Liu C, Wang J, Liu Y, Jiang S, Ren Z and Yin J: FGF5 promotes osteosarcoma cells proliferation via activating MAPK signaling pathway. Cancer Manag Res 11: 6457-6466, 2019.
30. Liu D, Zhang C, Li X, Zhang H, Pang Q and Wan A: MicroRNA-567 inhibits cell proliferation, migration and invasion by targeting FGF5 in osteosarcoma. EXCLI J 17: 102-112, 2018.
31. Fang F, Chang RM, Yu L, Lei X, Xiao S, Yang H and Yang LY: MicroRNA-188-5p suppresses tumor cell proliferation and metastasis by directly targeting FGF5 in hepatocellular carcinoma. J Hepatol 63: 874-885, 2015.
32. Kornmann M, Ishiwata T, Beger HG and Korc M: Fibroblast growth factor-5 stimulates mitogenic signaling and is overexpressed in human pancreatic cancer: Evidence for autocrine and paracrine actions. Oncogene 15: 1417-1424, 1997.